ELSEVIER

The Journal of Heart and Lung Transplantation

http://www.jhltonline.org

Machine-learning–based exploration to identify remodeling patterns associated with death or heart-transplant in pediatric-dilated cardiomyopathy

Patricia Garcia-Canadilla, PhD,[a,1] Sergio Sanchez-Martinez, PhD,[a,1] Pablo M. Martí-Castellote, MSc,[b] Cameron Slorach, RCDS,[c] Wei Hui, MD,[c] Gemma Piella, PhD,[b] Ainhoa M. Aguado, MSc,[a] Mariana Nogueira, PhD,[a] Luc Mertens, PhD,[c] Bart H. Bijnens, PhD,[a,d,1] and Mark K. Friedberg, MD[c,1]

From the [a]Institut d'Investigacions Biomèdiques August Pi i Sunyer (IDIBAPS) Barcelona, Spain; [b]BCN-MedTech, Universitat Pompeu Fabra, Barcelona, Spain; [c]Division of Cardiology, The Labatt Family Heart Center, Hospital for Sick Children, and University of Toronto, Toronto, Ontario, Canada; and the [d]ICREA, Barcelona, Spain.

KEYWORDS:
dilated cardiomyopathy;
pediatrics;
heart failure;
machine-learning;
echocardiography;
strain;
death;
heart transplantation

AIMS: We investigated left ventricular (LV) remodeling, mechanics, systolic and diastolic function, combined with clinical characteristics and heart-failure treatment in association to death or heart-transplant (DoT) in pediatric idiopathic, genetic or familial dilated cardiomyopathy (DCM), using interpretable machine-learning.

METHODS AND RESULTS: Echocardiographic and clinical data from pediatric DCM and healthy controls were retrospectively analyzed. Machine-learning included whole cardiac-cycle regional longitudinal strain, aortic, mitral and pulmonary vein Doppler velocity traces, age and body surface area. We used unsupervised multiple kernel learning for data dimensionality reduction, positioning patients based on complex conglomerate information similarity. Subsequently, k-means identified groups with similar phenotypes. The proportion experiencing DoT was evaluated. Pheno-grouping identified 5 clinically distinct groups that were associated with differing proportions of DoT. All healthy controls clustered in groups 1 to 2, while all, but one, DCM subjects, clustered in groups 3 to 5; internally validating the algorithm. Cluster-5 comprised the oldest, most medicated patients, with combined systolic and diastolic heart-failure and highest proportion of DoT. Cluster-4 included the youngest patients characterized by severe LV remodeling and systolic dysfunction, but mild diastolic dysfunction and the second-highest proportion of DoT. Cluster-3 comprised young patients with moderate remodeling and systolic dysfunction, preserved apical strain, pronounced diastolic dysfunction and lowest proportion of DoT.

CONCLUSIONS: Interpretable machine-learning, using full cardiac-cycle systolic and diastolic data, mechanics and clinical parameters, can potentially identify pediatric DCM patients at high-risk for

[1]These authors have contributed equally to this work.

Abbreviations: BSA, Body surface area; DCM, Dilated cardiomyopathy; DoT, Death or heart-transplant; ECG, Electrocardiogram; EF, Ejection fraction; IVRT, isovolumetric relaxation time; ICVT, isovolumic contraction time; LA, Left atrium; LV, Left ventricle; LVEDD, Left ventricular end-diastolic dimension; ML, Machine-learning; MKL, Multiple kernel learning; PV, Pulmonary vein; PW, Pulse-wave

Reprint requests: Mark K. Friedberg, MD, Hospital for Sick Children, 555 University Avenue, Toronto, ON, Canada, M5G 1 × 8. Telephone: +1-416-813-7239. Fax: +1-416-813-7548.

E-mail address: mark.friedberg@sickkids.ca

https://doi.org/10.1016/j.healun.2021.11.020

DoT, and delineate mechanisms associated with risk. This may facilitate more precise prognostication and treatment of pediatric DCM.
J Heart Lung Transplant 2022;41:516−526

Pediatric dilated cardiomyopathy (DCM) continues to carry high morbidity, heart-transplantation and death.[1,2] Therefore, accurate prognostication is important to guide clinical management. Echocardiography is commonly used in pediatric DCM management, as left ventricular (LV) remodeling, systolic, and diastolic function have been associated with the risk for DoT.[3-6]

It is difficult for the clinician to incorporate multiple parameters into a cohesive prognostic derivation, especially in children.[7] Moreover, useful information, such as patterns of segmental strain or blood-flow Doppler over the whole cardiac-cycle, are currently not quantified or integrated into assessment and prognostication. It is even more challenging to integrate these with clinical information to improve prognostication. Therefore, addressing this gap could have important clinical value.

Machine-learning (ML) can integrate and analyze large amounts of data. Specifically, similarity-based unsupervised ML allows for comparison of individuals, based on complex and heterogeneous data, including clinical, imaging parameters and complex imaging patterns over the cardiac-cycle duration. ML has been used in several settings and linked to prognosis.[8] However, never applied to pediatric DCM to improve and enrich risk-stratification for transplant-free survival.

We hypothesized that unsupervised ML, combining echocardiographic parameters, including complex patterns not traditionally analyzed, with clinical information, can help in understanding and predicting DoT. Using ML, we aimed to investigate the relationship of regional LV mechanics, global LV systolic and diastolic function, combined with clinical characteristics and heart failure medical treatment, to the outcomes of DoT in children with DCM.

Material and methods

Data from children, 0 to 18 years of age, diagnosed with idiopathic, familial or genetic DCM, presenting to our institution between 6/2004 (when digital echocardiography started) and 2016, were retrospectively analyzed. The study was approved by the institutional research ethics board with waiver of informed consent. We previously studied LV mechanics in this population.[9] Here, we present a more comprehensive and ML-based analysis of this cohort.

Inclusion criteria were a LV end-diastolic dimension (LVEDD) z-score>2 using institutional z-scores and a LV ejection fraction (EF) < 50%. Exclusion criteria included anatomic heart disease, pacing, mitral surgery, or LV noncompaction. The time of presentation (the initial time point) was considered as the first functional echocardiogram performed at presentation to our center. Follow-up duration was until death or heart transplant or study end in patients with transplant free-survival. Death could have been in or out of hospital. Transplant always occurred in hospital, at our center.

As an internal validation of the ML algorithm (i.e. to identify healthy patients as a separate cluster) and give context for the echo parameters and patterns in DCM patients overall, we analyzed a nonmatched control cohort of healthy volunteers who had normal medical history, physical examination, and echocardiogram.

Echocardiography was performed on General Electric (GE, Wauwatosa, Wisconsin) Vivid7 or E9 systems, with 5-12 MHz transducers according to patient size. To link between cardiac functional parameters, early in the clinical course, and outcomes, and as not to potentially bias associations by using an "end-stage" echocardiogram, the first study performed on the patient on a General Electric system was used for analysis. This was commonly the first echocardiogram obtained at the initial clinical assessment.

Clinical variables

Obtained from the medical record, included age, sex, weight, body surface area (BSA), heart-failure medications (diuretics, digoxin, beta-blockers, calcium-channel blockers, angiotensin converting enzyme inhibitors, and angiotensin receptor blockers) and 12-lead electrocardiogram (ECG) QRS duration.

Echocardiographic measurements included

Para-sternal short-axis LVEDD z-score, biplane modified Simpson's EF, aortic, mitral and pulmonary vein (PV) pulsed-wave (PW) Doppler and LV longitudinal strain from 3 septal and 3 lateral-wall segments obtained from the apical 4-chamber view.

Data processing

The operator extracting the digital traces from the images, and the operator entering the data into the ML algorithm were blinded to patient outcomes. The input for ML consisted of longitudinal strain and blood-pool velocities from the entire cardiac-cycle together with age and BSA. LV inflow and outflow and PV velocity images were manually segmented using a cloud-based platform.[10] A single cardiac-cycle was manually selected by indicating 2-consecutive onsets of the ECG QRS-complex. Then, landmarks on the velocity envelope were manually marked and interpolated using piecewise cubic splines to reconstitute the entire velocity trace. Valve opening and closing were defined for LV inflow and outflow traces, and S-wave onset for PV traces. Segmental LV longitudinal strain curves were derived from the 4-chamber apical view (Echopac, GE) and the values, over the whole cardiac-cycle, exported as text files. Strain and velocity profiles were then processed in MATLAB (R2020b, The MathWorks Inc., Natick, MA, 2020) as follows.

Temporal normalization

To allow quantitative inter-subject comparisons between traces with different heart-rates and timing of cardiac-phases, velocity profiles were temporally aligned, using valve opening and closure and onset of PV S-wave as temporal events, thereby ensuring alignment of isovolumetric contraction, systole, isovolumetric relaxation and

diastole.[11] A detailed description of the temporal normalization procedure can be found in the Supplementary Information.[12]

As temporal normalization may cause loss of time-related events associated with cardiac abnormalities, timing parameters used for alignment, including valve opening and closure, PV S-wave onset and heart-rate, were also considered in the learning. The combination of echocardiographic descriptors (regional strain and flow traces over the entire cardiac-cycle and temporal information) as well as age and BSA, yielded a total of 1015 data-points for each patient and defined the high-dimensional input for ML (Figure 1).

ML analysis

Unsupervised multiple kernel learning (MKL), a ML algorithm previously validated and extensively tested to analyze diverse echocardiographic data,[8,11,13] was used to quantify similarity between subjects, reduce data dimensionality and obtain a low-dimensional, easily interpretable, output space.[11] Finally, once positioned in the low-dimensional space, subjects were clustered using K-means (Figure 1) to identify phenotypically distinct groups of patients. A detailed description of the ML analysis can be found in the Supplementary Information.[8,11,13,14]

Statistical analysis

Continuous variables were expressed as mean ± standard deviation or median (25th-75th percentile) based on a normal distribution by Kolmogorov-Smirnov testing. Qualitative variables were expressed as a number and percentage. Differences between groups were analyzed for statistical significance using analysis of variance (ANOVA) for normally distributed variables and Kruskal-Wallis for non-normally distributed variables. A p value < 0.05 indicated statistical significance.

Results

Clinical characteristics

Forty-seven DCM (53% male; age 4.09 ± 5.5 years) and 25 healthy (44% male; age 8.23 ± 6.02 years) children were analyzed. Clinical characteristics of DCM transplant-free survivors vs nonsurvivors are shown in Table 1. Half the DCM cohort experienced DoT. Nonsurvivors had more diuretic and mechanical support use vs. survivors (Table 1).

Exploration of the low-dimensional output space

The MKL algorithm positioned DCM and healthy subjects in an output space based on similarity of echo data, along the duration of the cardiac-cycle, combined with age and BSA. Figures 2 & 3 show the resulting distribution (first 3 dimensions) of the individuals and how flow and strain patterns vary within the space. For ease of interpretation, aortic and mitral flows were combined to one "LV flow" trace, including the isovolumic phases. The left panels show individual positioning, with those that died or were transplanted indicated in red and clearly showing different positioning in the space, indicating that flows and strains are distinctly different. Examining the output space from above (dimension 1 vs 2; left panels Figures 2A and 3A, second from top), and investigating changes in dimension 1, patients located at the left-most region showed a normal pattern of LV and PV Doppler velocities (Figure 2A, brown traces) and strain (Figure 3A, brown traces). In comparison, patients located at the right-most region showed abnormal LV patterns consisting of: prolonged isovolumic contraction time (IVCT); reduced and late peaking aortic flow; prolonged isovolumetric relaxation (IVRT); decreased E and increased A; and mitral E-A fusion. PV flow showed later onset; a reduced S and D-waves; and increased A-wave reversal (AR) (Figure 2A, turquois traces). Similarly, deformation was severely reduced in all segments, most prominently in mid and base (Figure 3A, turquois traces). Dimension 2 (Figures 2B and 3B) shows predominantly timing differences in LV flow and reduced late S-wave PV velocities towards negative values (Figure 2B, brown traces). Deformation was overall reduced in all segments for negative coordinates in dimension 2 (Figure 3B, brown traces), with likely presence

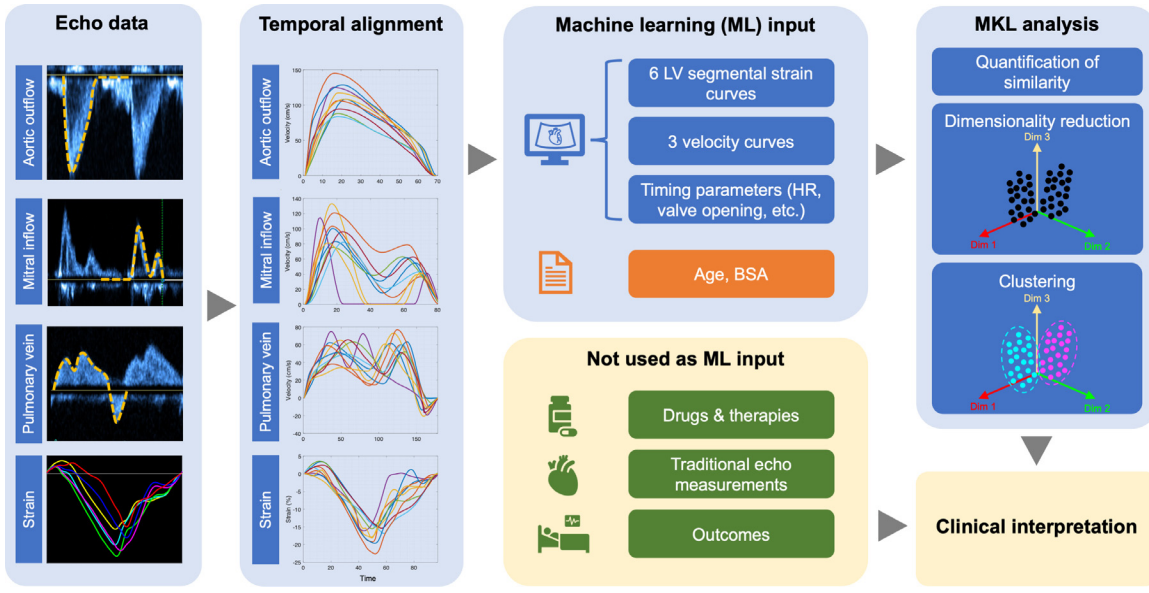

Figure 1 Schematic representation of the pipeline for data processing and machine-learning analysis. BSA, Body surface area; Dim, dimension; HR, heart rate; LV, left ventricle.

Table 1 Clinical and Classical Echo Characteristics of Transplant-Free Survival vs Death or Transplant Cohorts

	Transplant-free survival (N = 23)	Death or transplant (N = 24)	*p* value
Female sex	10 (43.48%)	12 (50%)	0.6542
Age (years)	0.5 (0.16-3.86)	0.61 (0.28-10.9)	0.3382
Weight (Kg)	7 (4.95-15.48)	7.45 (5.85-36.5)	0.4958
BSA (m^2)	0.36 (0.29-0.67)	0.38 (0.32-1.2)	0.4496
QRS duration (ms)	80.26 ± 23.37	79 ± 21.3	0.8475
LVEF	26.65 ± 8.13	19.67 ± 7.78	0.0043
LVEDD z-score	6.59 ± 2.71	8.43 ± 3.97	0.0714
GLS (%)	-6.88 ± 3.75	-5.96 ± 3.07	0.3593
Medications			
Diuretics	13 (56.52%)	22 (91.67%)	0.0057
ACE-I	12 (52.17%)	17 (70.83%)	0.1884
B-Blockers	11 (47.83%)	11 (45.83%)	0.8911
MRA	6 (26.09%)	4 (16.67%)	0.4302
Digoxin	2 (8.7%)	1 (4.17%)	0.5255
Inotropes	2 (8.7%)	7 (29.17%)	0.0746
Antiarrhythmic	2 (8.7%)	3 (12.5%)	0.6724

ACE-I, Angiotensin converting enzyme inhibitors; BSA, body surface area; GLS, global longitudinal strain; LVEDD, left ventricular end-diastolic dimension; LVEF, left ventricular ejection fraction; MRA, mineralocorticoid inhibitors.

of post-systolic deformation. Examining the space from the left (dimension 1 vs 3; left panels Figures 2C and 3C, bottom), and investigating changes in dimension 3, IVCT was prolonged with late peaking aortic flows. Patients located at the bottom-most region had short IVRT, high E-velocities with fast deceleration and low A-velocities, while at the same time PV flow showed reduced S and increased D-waves velocities together with a delayed and prolonged AR-wave, of much longer duration than the mitral A-wave (Figure 2C, brown traces). At the same time, deformation was only mildly reduced overall, without regional changes (Figure 3C, brown traces). In comparison, patients located at the top-most region showed (beyond a long IVCT and late peaking aortic flow) a long IVRT, reduced E with increased A and mitral E-A fusion (Figure 2C, turquois traces) and reduced basal strain with apical sparing (Figure 3C, turquois traces).

Unsupervised clustering

Clustering on the 7 first dimensions of the low-dimensional space resulted in 5-clusters with significantly different proportions of DoT (Table S1). These were clinically relevant in relation to conventional echo parameters that were not used for learning. All controls localized in cluster-1 and 2, while all, but one, DCM subjects localized in clusters-3, 4 and 5. The clinical characteristics and the corresponding representative LV velocity and strain traces, are shown for each cluster in Figure 4.

The clusters containing the controls (Figure 4, dark and light green) showed normally shaped flows and strain traces and differentiated predominantly in age (with cluster-1 containing the youngest and cluster-2 containing the oldest healthy subjects) and age-related heart-rate (higher in youngest—Figure 4E). As seen in Figure 4A, one DCM patient who experienced transplant was classified with healthy subjects. This individual is located near another isolated individual with the same poor outcome but classified in cluster-5. For this individual, the time between the echocardiographic exam and outcome was much larger than average (1216 vs 180.5 days).

Clusters 3 to 5 only contained DCM patients. When comparing the information used during learning, the following observations can be made regarding blood-flow velocities (Figure 4C,D):

- All DCM clusters show prolonged IVCT.
- Clusters 3 and 4 show a prolonged ejection time with late peaking aortic flow, while this is less prominent in Cluster-5.
- Clusters 3 and 4 show prolonged IVRT with E-A fusion in cluster-4, while cluster-5 shows a much shorter IVRT with rapid and short E.
- Examining PV flow, all DCM clusters have a decreased S-wave, most prominent in cluster-5, which also shows a higher D compared to S-wave. All 3-clusters have increased AR-wave amplitude with cluster-3 and (even more prominently in) cluster-5 showing marked prolongation of PV AR-wave as compared to the mitral A-wave (quantified in Figure 4F).

LV strains showed the following characteristics for the 3 DCM clusters (Figure 4G):

- Globally, all segments show lower deformation in all DCM patients.
- Cluster-3 predominantly shows decreased strain in the basal-mid septum, with post-systolic deformation in these regions.
- Cluster-4 shows severely reduced basal strain with some apical sparing.
- Cluster-5 shows overall reduced strain with some apical sparing.

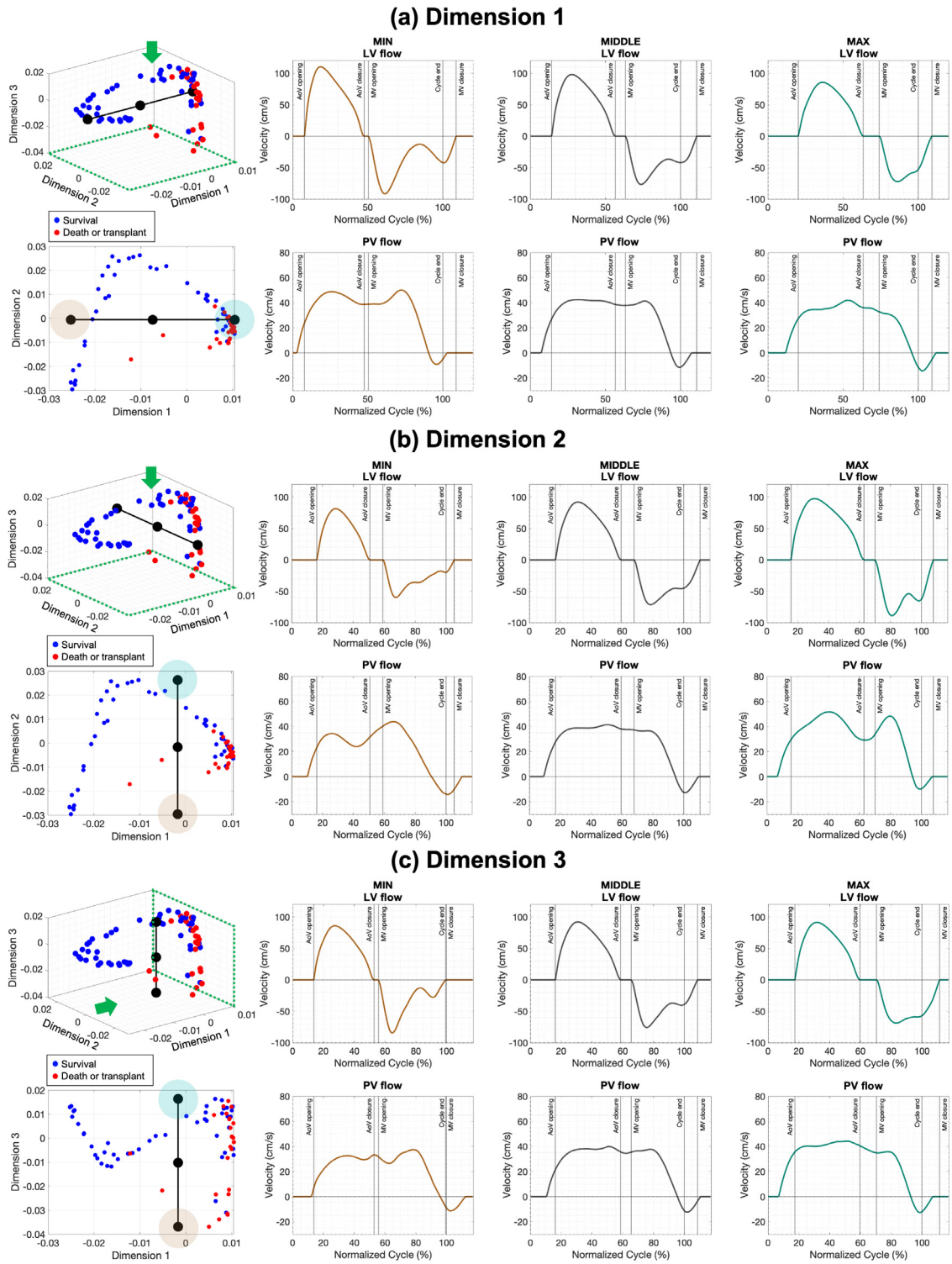

Figure 2 Exploration of the low-dimensional output space. (Left) The left panels of the figures show the positioning of the individuals in the (3 first dimensions) of the output space, with those who dies or were transplanted in red, and the point-of-view (green arrow) for the 2-dimensional representation of the output space. (Right) Exploration of the (A) first, (B) second, and (C) third dimensions of LV echo data variability. Aortic, mitral and PV velocity curves corresponding to the regions marked by the 3 black dots, corresponding to the minimum (brown), middle (black) and maximum (turquoise) positions along each dimension were plotted. Aortic and mitral velocities (ignoring any regurgitation that might be present) are combined to one "LV flow" trace, including the isovolumic phases.

When investigating the clusters for outcome and clinical variables not used for the learning, the following observations can be made (Figure 4B, Table S1):

The cluster with the highest proportion of death or transplant (cluster-5) comprised the oldest individuals treated most intensively with heart-failure medications. They had the largest left atria (LA) volumes and were further characterized by reduced deformation, prolonged IVCT, reduced, shortened and late peaking outflow, indicating systolic dysfunction. Additionally, the short

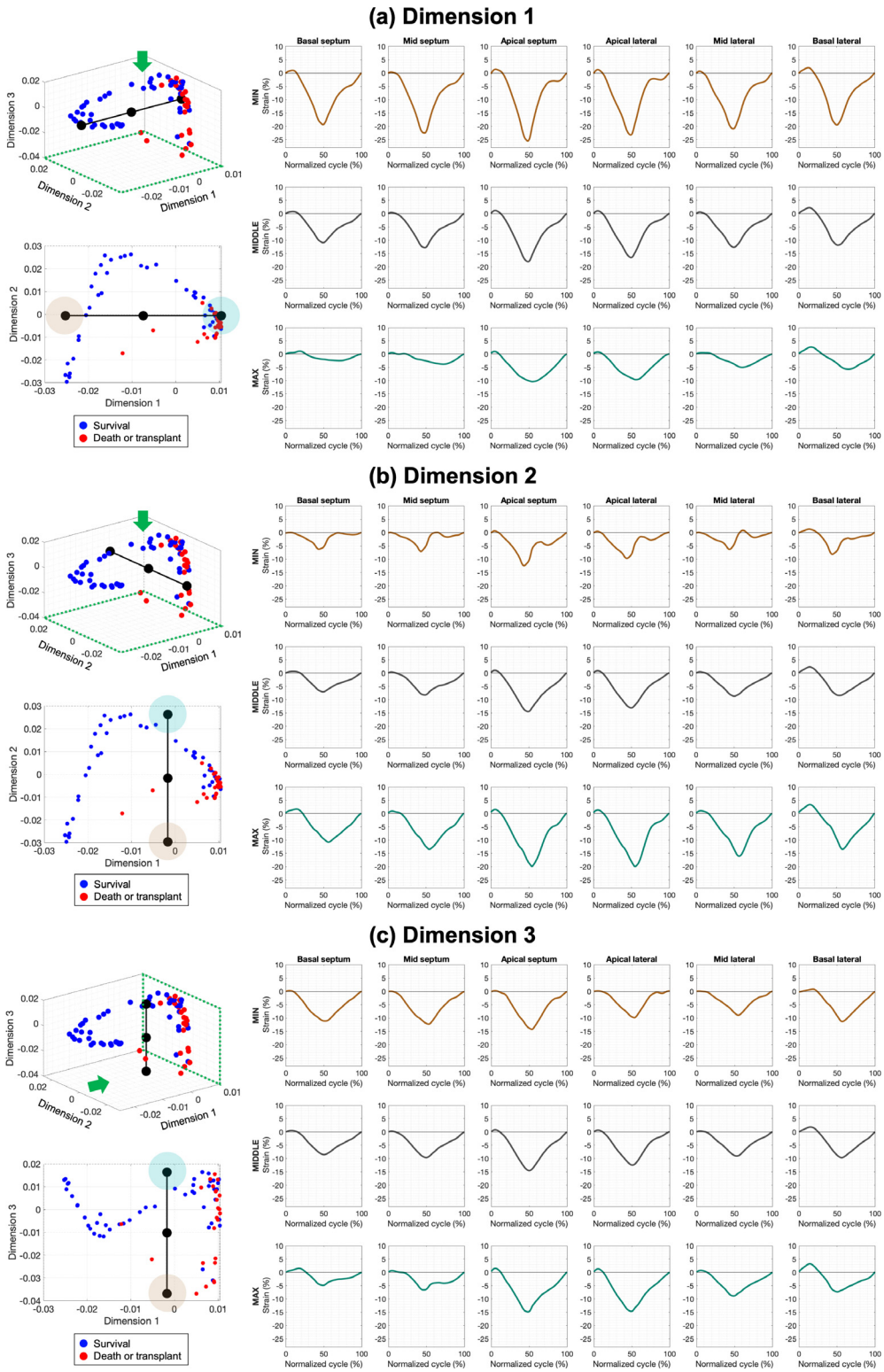

Figure 3 Exploration of the low-dimensional output space. (Left) The left panels of the figures show the positioning of the individuals in the (3 first dimensions) of the output space, with those who dies or were transplanted in red, and the point-of-view (green arrow) for the 2-dimensional representation of the output space. (Right) Exploration of the (A) first, (B) second, and (C) third dimensions of LV deformation data variability. LV deformation curves corresponding to the regions marked by the 3 black dots corresponding to the minimum (brown), middle (black) and maximum (turquoise) positions along each dimension were plotted.

IVRT, preserved E-wave with decreased A-wave, lowest PV S-wave velocities (Figure 4D), largest time-difference between end of AR-wave and end of mitral A-wave (Figure 4F) and largest LA volume (Table S1), indicate important diastolic dysfunction. These findings suggest globally failing hearts.

The cluster with the second highest proportion of death or transplant (cluster-4) compromised young DCM subjects

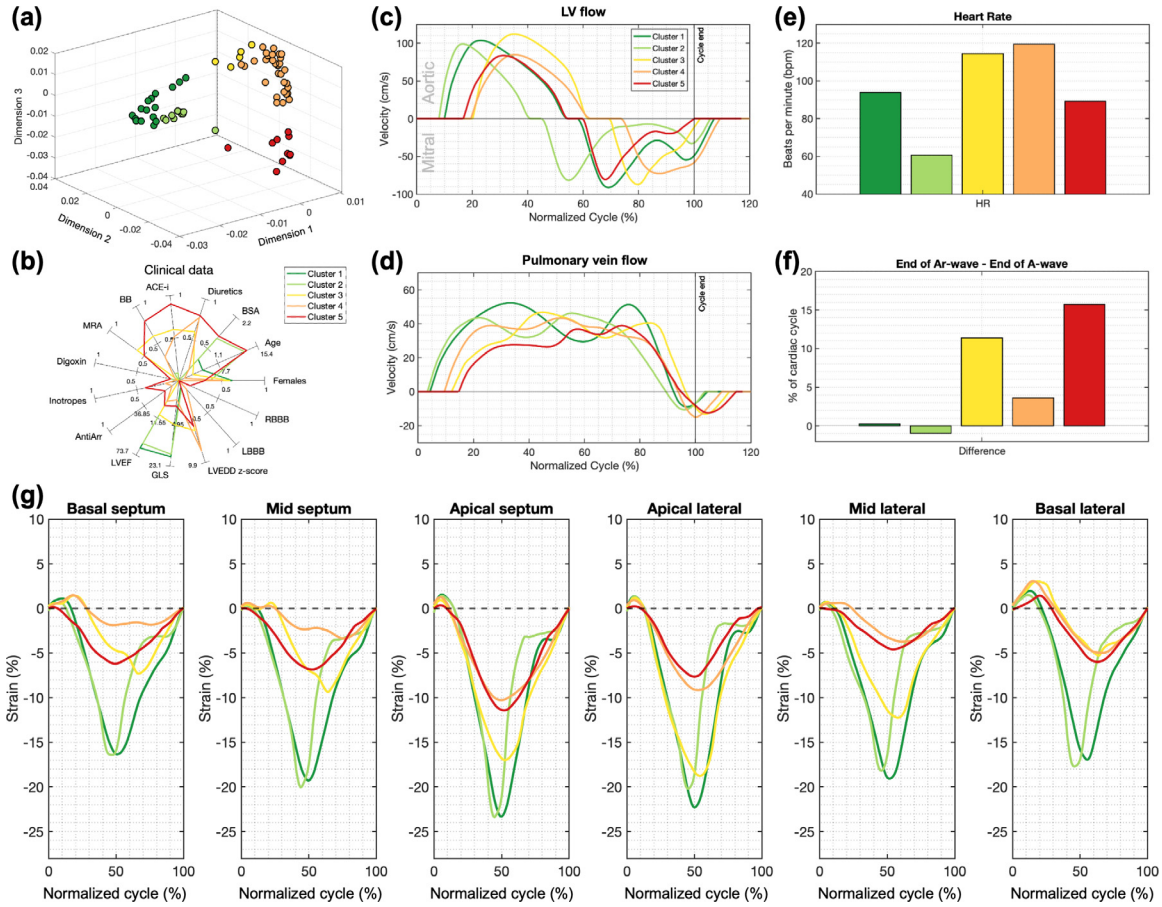

Figure 4 The "fingerprints" of clinical characteristics as well as the corresponding representative LV velocity and longitudinal strain traces. (A) Cluster distribution in the first 3 dimensions of the low-dimensional output space. (B) Clinical and conventional echo characteristics of each cluster. Representative (C) LV velocity traces, (D) pulmonary vein velocity traces, (E) heart rate, (F) time difference (in percentage) between the end of the PV AR and mitral A-waves, and (G) LV deformation traces of each cluster.

with the lowest LVEF and GLS and highest LVEDD z-score, but with normal LA size (Table S1). This group also had the most reduced and delayed peak aortic outflow velocity, and most reduced basal and mid deformation (Figure 4G), indicating severe systolic dysfunction. They had the shortest filling time, highest heart-rate with mitral E-A fusion, but longest IVRT, with very little prolongation of the PV AR-wave as compared to mitral A-wave duration and normal LA size (Table S1). These findings suggest milder diastolic dysfunction with low filling-pressures.

Finally, cluster-3 comprised young DCM subjects with the lowest risk of death or transplant, moderately reduced LVEF and GLS and moderately enlarged LVs and LAs. They had prolonged IVCT, but high and normal peaking aortic outflow, decreased deformation in basal segments (with marked septal post-systolic shortening—Figure 4G), and near-normal apical strains, all suggestive of moderate systolic dysfunction. They showed only slightly increased IVRT, moderate mitral E-A fusion, but overall the shortest filling time (Figure 4C), and low PV S-wave velocities (Figure 4D) and a large difference between the PV AR-wave and mitral A-wave durations (Figure 4F) and enlarged LA (Table S1), consistent with predominant LV diastolic dysfunction.

Figure 5 summarizes the main clinical characteristics, echocardiographic patterns and outcomes of each cluster.

Discussion

DCM carries high morbidity and mortality in children with little improvement in survival.[1] In this proof-of-concept study we investigated the usefulness of combining echocardiographic parameters of regional mechanics, diastolic parameters and LV outflow Doppler characteristics (as reflecting LV pump function), over the cardiac cycle, with clinical characteristics, to understand the spectrum of remodeling in pediatric DCM. The results show that by combining these parameters, ML can cluster patients into distinct groups with different proportions of DoT. Our results suggest that this approach may further our understanding of underlying LV remodeling process, and which parameters are associated with more DoT in pediatric DCM. To our knowledge, this is the first time this approach has been published in pediatric DCM.

Many of the echo and clinical parameters entered into the ML model, are known to be associated with transplant-free survival or the risk for disease progression but have not been integrated.[3-5,15,16] As opposed to assessing the

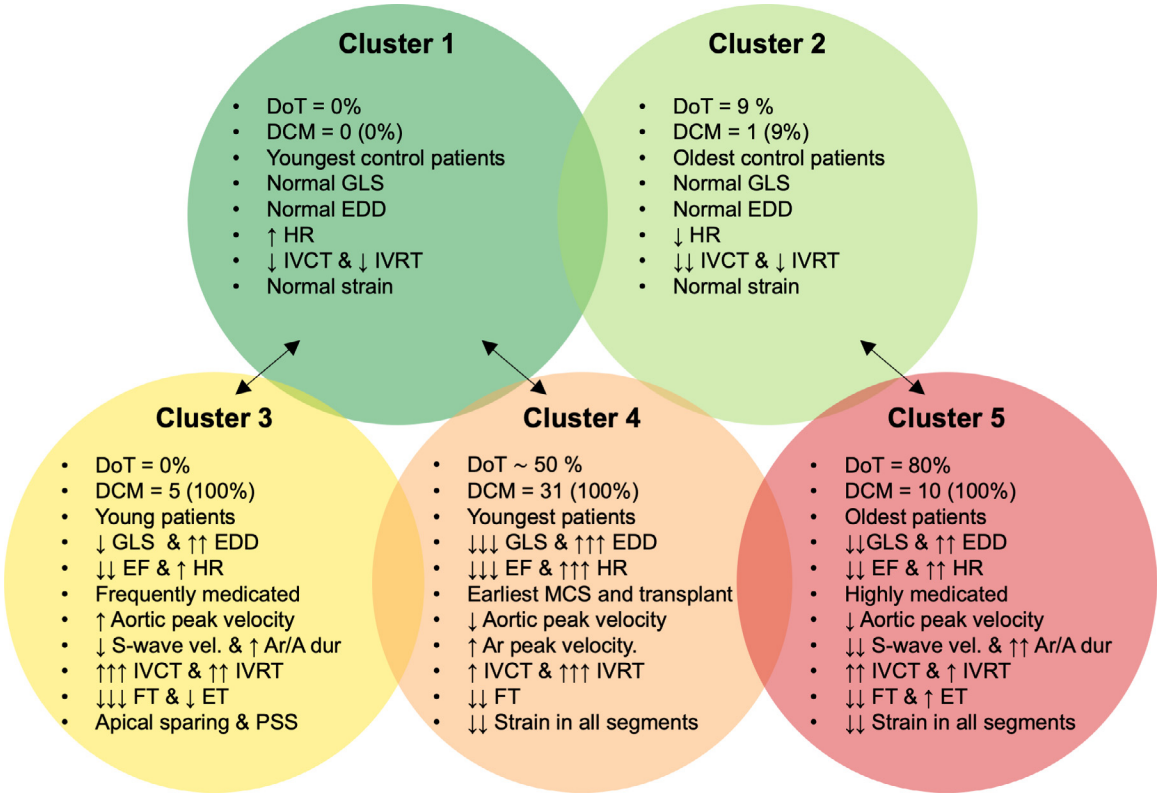

Figure 5 Typical clinical characteristics, features of left ventricular echo and deformation patterns and outcome rates of the 5 phenogroups. The green circles represent the 2 clusters that contain all the healthy subjects, while yellow, orange, and red circles represent the 3 clusters containing all the DCM subjects but one. DCM, dilated cardiomyopathy; DoT, death or transplant; EDD, end-diastolic diameter; EF, ejection time; FT, filling time; GLS, global longitudinal strain; HR, heart rate; ICRT, isovolumetric relaxation time; IVCT, isovolumetric contraction time; MCS, mechanical support; PSS, postsystolic shortening.

predictive value of individual parameters, our approach positions individuals with regards to each other based on similarity in cardiac-cycle wide deformation and (aortic/mitral/PV) flow patterns. This incorporates routine parameters as well as their unique characteristics over the duration of the cardiac-cycle that are not usually analyzed. Moreover, it integrates aspects of ejection and filling. This approach approximates what physicians strive for: to synthesize all available information into a comprehensive assessment. However, it is difficult, if not impossible, for the human brain to incorporate and synthesize multiple data simultaneously in an unbiased manner.

From the positioning of individuals in relation to each other, several observations can be made on pathophysiological changes in the failing pediatric heart. Given that we analyze cycle-wide flows, we can observe variability in aortic outflow, where a longer IVCT and a decreased and delayed outflow velocity was seen in high-risk clusters. In the normal LV, when contractility and loading are balanced, aortic outflow peaks around one third of the ejection period; and then gradually decreases, corresponding to decreased force development. When loading is disproportionally increased or contractility impaired,[17] force-development prolongs, resulting in late peaking outflow velocities with a rounded rather than triangular profile. Similarly, mitral Doppler patterns showed well-known changes associated with filling abnormalities, such as alterations in IVRT, E-wave peak and deceleration, A-wave contribution and heart-rate-related fusion, over and above absolute peak E and A values. It is notable, however, that although the A-wave becomes more dominant when IVRT lengthens, and decreases again in patients with worse prognosis, where IVRT is shorter and deceleration time tends to be shorter, this is far less impressive compared to patterns observed during pseudonormalization or restriction in adults, consistent with our observations that pediatric diastolic changes do not follow adult patterns.[7] The timing and duration of ejection and filling are clearly important, consistent with the systolic:diastolic duration ratio being associated with DoT in pediatric DCM.[18]

PV Doppler analysis also showed interesting observations. Although there is a tendency towards lower S-waves and increased D-waves with worse outcome, these changes are less marked compared to adult heart-failure.[19,20] In contrast, PV AR-wave duration and its relation to mitral A-wave duration, are relevant in relation to outcome. Given that PV AR-wave prolongation appears concomitantly with shortened IVRT, this suggests elevated atrial pressures.[20,21] Our findings suggest that a comprehensive assessment of Doppler traces and their patterns (including mitral, PV and LV outflow) is important, over and above singular measurements of peak velocities.[7]

In addition to flow patterns, we incorporated regional deformation along the full cardiac cycle. We previously showed that timing of peak strain,[22] its segmental dispersion, as well as the "global" pattern of strain over the LV,[23]

are associated with function and possibly clinical outcomes in pediatric DCM.[9,24] Here, we additionally show that different patterns occur, some of which associated with higher risk. Whereas a global and severe decrease in deformation in all segments is associated with worse outcome, we observe that changes in basal segments are specifically important and may be more sensitive compared to GLS.

As opposed to the classical approach where single variables are used for classifying findings, our proposed phenogrouping identified different remodeling profiles associated with differing proportions of DoT. The group with the highest proportion of DoT (cluster-5) were characterized by findings that suggest globally failing hearts, explaining their high risk.

Conversely, the group with the second highest proportion of DoT (cluster-4) was characterized by severe systolic but relatively mild diastolic dysfunction. Interestingly,

Cluster 3 comprised of young DCM subjects with lowest risk of DoT while they had findings suggestive of predominant LV diastolic dysfunction with only moderate systolic dysfunction.

Previous literature suggests that the youngest patient populations with DCM have the worst outcomes with another increase during adolescence. However, some large registries have suggested that older age is associated with worse outcome.[2] This apparent controversy clearly indicates that age itself is likely not the determining factor, as can also be seen from our data (Table 1), showing that the age was similar between DCM patients with vs without an outcome. While our sample is too small vs much larger registries to determine that younger children have similar or better outcomes compared to older children, our novel approach might provide more insight into this controversy by showing that it is the phenotype, potentially independent of age, that would determine outcome. We see on both age groups that those with more systolic dysfunction were positioned in clusters that had more risk of adverse outcome while predominantly diastolic dysfunction seems better controllable. To better illustrate the age distribution in our population and clusters, we have constructed histograms of the patient's age in the different clusters and have added this to the supplementary material (Supplementary Figure S1). The histogram clearly shows 2 age groups, a very young and a more adolescent group.

Our results suggest that integrating cardiac mechanics and hemodynamics surpasses the potential of "traditional" statistics on a set of individual measurements. Our results may further provide new insights into the pathophysiology of pediatric heart-failure including (predominant) diastolic dysfunction.

One may question whether combining "raw information" from which well-tested parameters are extracted is needed. Based on current results, we believe it is. For example, although it is widely accepted that diastolic dysfunction is associated with clinical outcomes, this has been difficult to demonstrate systematically in pediatric DCM.[7] Here we show that more subtle changes of abnormal relaxation are present combined with signs of elevated filling-pressures in those at highest risk.

The use of artificial intelligence is evolving, predominantly in adult studies, using "big-data" and unsupervised ML approaches to classify phenotypes who may be treated similarly, with a predictable response.[25] Unbiased or unsupervised hierarchical clustering has been used to identify new phenotypes in cohorts of adults with heart failure.[26,27] Our approach could foreseeably be utilized in the same way in the phenotypically heterogeneous pediatric population. Our results will need to be validated in larger studies.[28] In large adult studies, clusters could be defined by severity of ventricular function, or etiology, in relation to RNA-sequenced distinct gene expression profiles.[25] Our approach may address more directly the pathophysiology and perhaps mechanism of the expressed phenotype, which may also be useful to guide treatment. While our study cannot answer this question, the lack of effective medical treatment in pediatric DCM makes this very relevant. Cluster-3 was characterized by young patients, all of whom survived without transplant, with a high proportion of early medical treatment. In contrast, cluster-5 was characterized by older patients with a very high rate of DoT, and frequent medication. This questions use of similar medications in different age groups and disease characteristics. While ML phenogrouping may be used in the future to predict response to medication and hence guide the choice of medications, the current study, due to its retrospective design and the impact of the clinician in determining the medical treatment, cannot determine changes in patient features and/or prognosis based on medical therapy. This would necessitate prospective studies.

While our proposed approach shows potential for assessing prognosis, and clearly shows the underlying etiologies associated with the patient's clinical presentation and thus contributing to a better understanding, prospective as well as serial validation studies are needed. If confirmed by such studies, one may envision ML algorithms embedded in echocardiography or medical record platforms. That, instead of only list image-based measurements, integrate hemodynamic Doppler, functional and strain data and clinical characteristics to provide an "online" assessment tool that the clinician may use to phenotype patients in real time for risk assessment and to improve prognostication. Ultimately, these comprehensive and integrated tools may also be used to predict the chance of response to medications; or use lack of a response as an additional predictive parameter. This may substantially refine and improve the medical therapeutic approaches, need for transplantation and/or potentially the timing of mechanical circulatory support placement.

Limitations

This is a relatively small cohort from a single center. There are other multiple relevant parameters that were not included during the learning, for example biomarkers and genotype. One of the main limitations is the lack of a validation cohort. When using ML approaches for classification, independent validation, using internal cross validation,

as well as external validation with other cohorts, is important to avoid overfitting and to provide a reliable predictor. This initial study serves as proof of principle, while at the same time providing interpretable insights into the pathophysiological changes in cardiac mechanics and hemodynamics in pediatric DCM. The unsupervised phenogrouping avoids bias based on outcome of diagnostic labels. However, comprehensive validation is needed.

Conclusion

In conclusion, this exploratory study shows the potential of (unsupervised) ML to integrate comprehensive echo and clinical data for phenotyping and risk stratification in pediatric DCM. Our initial results seem to identify subgroups with varying degrees of systolic and diastolic dysfunction, associated with variable risks, which can form the basis to investigate larger samples, including comprehensive validation in separate cohorts.

Author contributions

MF, LM, BB conceived and designed the analysis.

CS, WH collected the data.

PGC, SSM, PMC, AA, MN, GP contributed data or analysis tools.

PGC, SSM, PMC, BB performed the analysis.

PGC, BB, MF wrote the paper.

All authors discussed contributed to the final manuscript.

Disclosure statement

The authors report no conflict of interest.

Patricia Garcia-Canadilla has received funding from the postdoctoral fellowships program Beatriu de Pinos (2018-BP-00201), funded by the Secretary of Universities and Research (Goverment of Catalonia) and by the Horizon 2020 programme of research and innovation of the European Union under the Marie Skłodowska-Curie grant agreement N° 801370. Pablo Miki Martí-Castellote has received funding from the predoctoral fellowships program FI-SDUR (2020-FISDU-00169) from AGAUR.

Supplementary materials

Supplementary material associated with this article can be found in the online version at https://doi.org/10.1016/j.healun.2021.11.020.

References

1. Lipshultz SE, Law YM, Asante-Korang A, et al. Cardiomyopathy in children: classification and diagnosis: a scientific statement from the American Heart Association. Circulation 2019;140:E9-E68. https://doi.org/10.1161/CIR.0000000000000682.
2. Towbin JA, Lowe AM, Colan SD, et al. Incidence, causes, and outcomes of dilated cardiomyopathy in children. J Am Med Assoc 2006;296:1867-76. https://doi.org/10.1001/jama.296.15.1867.
3. Ishii R, Steve Fan CP, Mertens L, Manlhiot C, Friedberg MK. Longitudinal prediction of transplant-free survival by echocardiography in pediatric dilated cardiomyopathy. Can J Cardiol 2021. https://doi.org/10.1016/j.cjca.2020.12.010. Published online.
4. van der Meulen M, den Boer S, du Marchie Sarvaas GJ, et al. Predicting outcome in children with dilated cardiomyopathy: the use of repeated measurements of risk factors for outcome. ESC Heart Fail 2021;8:1472-81. https://doi.org/10.1002/ehf2.13233.
5. Alvarez JA, Orav EJ, Wilkinson JD, et al. Competing risks for death and cardiac transplantation in children with dilated cardiomyopathy: results from the pediatric cardiomyopathy registry. Circulation 2011;124:814-23. https://doi.org/10.1161/CIRCULATIONAHA.110.973826.
6. Foerster SR, Canter CE, Cinar A, et al. Ventricular remodeling and survival are more favorable for myocarditis than for idiopathic dilated cardiomyopathy in childhood: an outcomes study from the pediatric cardiomyopathy registry. Circ Heart Fail 2010;3:689-97. https://doi.org/10.1161/CIRCHEARTFAILURE.109.902833.
7. Dragulescu A, Mertens L, Friedberg MK. Interpretation of left ventricular diastolic dysfunction in children with cardiomyopathy by echocardiography. Circ Cardiovasc Imaging 2018;6:254-61. https://doi.org/10.1161/circimaging.112.000175.
8. Cikes M, Sanchez-Martinez S, Claggett B, et al. Machine learning-based phenogrouping in heart failure to identify responders to cardiac resynchronization therapy. Eur J Heart Fail 2019;21:74-85. https://doi.org/10.1002/ejhf.1333.
9. Forsha D, Slorach C, Chen CK, et al. Patterns of mechanical inefficiency in pediatric dilated cardiomyopathy and their relation to left ventricular function and clinical outcomes. J Am Soc Echocardiogr 2016;29:226-36. https://doi.org/10.1016/j.echo.2015.11.011.
10. Rocket viewer. 2018. Available at: https://github.com/bcn-medtech/rocket_viewer Accessed May 17, 2021.
11. Sanchez-Martinez S, Duchateau N, Erdei T, et al. Machine learning analysis of left ventricular function to characterize heart failure with preserved ejection fraction. Circ Cardiovasc Imaging 2018;11:1-12. https://doi.org/10.1161/CIRCIMAGING.117.007138.
12. Duchateau N, Giraldeau G, Gabrielli L, et al. Quantification of local changes in myocardial motion by diffeomorphic registration via currents: application to paced hypertrophic obstructive cardiomyopathy in 2D echocardiographic sequences. Med Image Anal 2015;19:203-19. https://doi.org/10.1016/j.media.2014.10.005.
13. Sanchez-Martinez S, Duchateau N, Erdei T, Fraser AG, Bijnens BH, Piella G. Characterization of myocardial motion patterns by unsupervised multiple kernel learning. Med Image Anal 2017;35:70-82. https://doi.org/10.1016/j.media.2016.06.007.
14. Sanchez-Martinez S. Unsupervised multiple kernel learning. Available at: https://github.com/bcnmedtech/unsupervised_multiple_kernel_learning Accessed May 17, 2021.
15. Molina KM, Shrader P, Colan SD, et al. Predictors of disease progression in pediatric dilated cardiomyopathy. Circ Heart Fail 2013;6:1214-22. https://doi.org/10.1161/circheartfailure.113.000125.
16. den Boer SL, du Marchie Sarvaas GJ, Klitsie LM, et al. Longitudinal strain as risk factor for outcome in pediatric dilated cardiomyopathy. JACC Cardiovasc Imaging 2016;9:1121-2. https://doi.org/10.1016/j.jcmg.2015.10.008.
17. Cikes M, Kalinic H, Baltabaeva A, et al. The shape of the aortic outflow velocity profile revisited: is there a relation between its asymmetry and ventricular function in coronary artery disease? Eur J Echocardiogr 2009;10:847-57. https://doi.org/10.1093/ejechocard/jep088.
18. Mondal T, Slorach C, Manlhiot C, et al. Prognostic implications of the systolic to diastolic duration ratio in children with idiopathic or familial dilated cardiomyopathy. Circu Cardiovasc Imaging 2014;7:773-80. https://doi.org/10.1161/circimaging.114.002120.
19. Güvenç TS, Poyraz E, Çetin Güvenç R, Can F. Contemporary usefulness of pulmonary venous flow parameters to estimate left ventricular end-diastolic pressure on transthoracic echocardiography. Int J Cardiovasc Imaging 2020;36:1699-709. https://doi.org/10.1007/s10554-020-01886-6.

20. Lester SJ, Tajik AJ, Nishimura RA, Oh JK, Khandheria BK, Seward JB. Unlocking the mysteries of diastolic function. Deciphering the Rosetta stone 10 years later. J Am Coll Cardiol 2008;51:679-89. https://doi.org/10.1016/j.jacc.2007.09.061.
21. Nagueh SF, Smiseth OA, Appleton CP, et al. Recommendations for the evaluation of left ventricular diastolic function by echocardiography: an update from the American Society of Echocardiography and the European Association of Cardiovascular Imaging. J Am Soc Echocardiogr 2016;29:277-314. https://doi.org/10.1016/j.echo.2016.01.011.
22. Friedberg MK, Slorach C. Relation between left ventricular regional radial function and radial wall motion abnormalities using two-dimensional speckle tracking in children with idiopathic dilated cardiomyopathy. Am J Cardiol 2008;102:335-9. https://doi.org/10.1016/j.amjcard.2008.03.064.
23. Friedberg MK, Roche SL, Balasingam M, et al. Evaluation of mechanical dyssynchrony in children with idiopathic dilated cardiomyopathy and associated clinical outcomes. Am J Cardiol 2008;101:1191-5. https://doi.org/10.1016/j.amjcard.2007.12.017.
24. Forsha D, Slorach C, Chen CK, et al. Classic-pattern dyssynchrony and electrical activation delays in pediatric dilated cardiomyopathy. J Am Soc Echocardiogr 2014;27:956-64. https://doi.org/10.1016/j.echo.2014.06.014.
25. Verdonschot JAJ, Merlo M, Dominguez F, et al. Phenotypic clustering of dilated cardiomyopathy patients highlights important pathophysiological differences. Eur Heart J 2020;42:ehaa841. https://doi.org/10.1093/eurheartj/ehaa841.
26. Shah SJ, Katz DH, Selvaraj S, et al. Phenomapping for novel classification of heart failure with preserved ejection fraction. Circulation 2015;131:269-79. https://doi.org/10.1161/CIRCULATIONAHA.114.010637.
27. Segar MW, Patel KV, Ayers C, et al. Phenomapping of patients with heart failure with preserved ejection fraction using machine learning-based unsupervised cluster analysis. Eur J Heart Fail 2020;22:148-58. https://doi.org/10.1002/ejhf.1621.
28. Merlo M, Pivetta A, Pinamonti B, et al. Long-term prognostic impact of therapeutic strategies in patients with idiopathic dilated cardiomyopathy: changing mortality over the last 30 years. Eur J Heart Fail 2014;16:317-24. https://doi.org/10.1002/ejhf.16.